Synthesis, Structure, and Spectroscopic and Electrochemical Properties of Heteroleptic Bis(phthalocyaninato) Rare Earth Complexes with a C_4 Symmetry

by **Yongzhong Bian**[a]), **Rongming Wang**[a]), **Daqi Wang**[b]), **Pehua Zhu**[a]), **Renjie Li**[a]), **Jianmin Dou**[b]), **Wei Liu**[a]), **Chi-Fung Choi**[c]), **Hoi-Shan Chan**[c]), **Changqin Ma***[a]), **Dennis K. P. Ng***[c]), and **Jianzhuang Jiang***[a])

[a]) Department of Chemistry, Shandong University, Jinan 250100, China (e-mail: jzjiang@sdu.edu.cn)

[b]) Department of Chemistry, Liaocheng University, Liaocheng 252000, China

[c]) Department of Chemistry, The Chinese University of Hong Kong, Shatin, N.T., Hong Kong, China (e-mail: dkpn@cuhk.edu.hk)

A series of eleven heteroleptic bis(phthalocyaninato) rare earth double-deckers $[M^{III}(pc)\{pc(\alpha\text{-}OC_5H_{11})_4\}]$ **1**–**11** (M = Y, Sm–Lu; pc = phthalocyaninato; $pc(\alpha\text{-}OC_5H_{11})_4$ = 1,8,15,22-tetrakis(1-ethylpropoxy)phthalocyaninato) were prepared as racemic mixtures by $[M^{III}(pc)(acac)]$-induced (acac = acetylacetonato) cyclic tetramerization of 3-(1-ethylpropoxy)phthalonitrile in the presence of 1,8-diazabicyclo[5.4.0]undec-7-ene (DBU) in refluxing pentanol. These compounds could also be prepared by treating $[M^{III}(pc)(acac)]$ with the metal-free phthalocyanine $H_2\{pc(\alpha\text{-}OC_5H_{11})_4\}$ in refluxing octanol. The whole series of double-decker complexes **1**–**11** were characterized by elemental analysis and various spectroscopic methods. The molecular structures of the Sm, Eu, and Er complexes **1**, **2**, and **8**, respectively, were also determined by single-crystal X-ray diffraction analysis. The effects of the rare earth ion size on the reaction yield, molecular structure, and spectroscopic and electrochemical properties of these complexes were systematically examined.

Introduction. – There has been a growing interest in optically active tetrapyrrole derivatives because of their biological relevance and various potential applications [1]. While chiral porphyrins, ranging from synthetic to naturally occurring analogues, have been extensively studied over the past few decades (for some recent examples, see [2]), the phthalocyanine counterparts have only been reported recently [3]. Because of the unique structure, sandwich-like rare earth complexes [4] with certain tetrapyrrolato ligands can exhibit chirality. Chiral bis(tetrapyrrolato) complexes, however, remain extremely rare so far. *Aida* and co-workers have recently reported the optical resolution and racemization of chiral bis(porphyrinato)cerium compounds with a D_2 symmetry [5]. These complexes have also been used as receptors for metal ions, dicarboxylic acids, and saccharides through positive homotropic allosterism [6]. Recently, *Simon* and co-workers have briefly reported a racemic mixture of $[Lu^{III}(pc)(nc^*)]$ (pc = phthalocyaninato; nc* = C_s isomer of 1,2-naphthalocyaninato), the structure of which has been inferred from ^{1}H-NMR data [7].

We describe herein a detailed and systematic study of a novel series of the eleven heteroleptic bis(phthalocyaninato) rare earth complexes $[M^{III}(pc)\{pc(\alpha\text{-}OC_5H_{11})_4\}]$ **1**–**11** (M = Y, Sm–Lu); $pc(\alpha\text{-}OC_5H_{11})_4$ = 1,8,15,22-tetrakis(1-ethylpropoxy)phthalocyaninato (see *Fig. 1*), including their structures, spectroscopic properties, and electro-

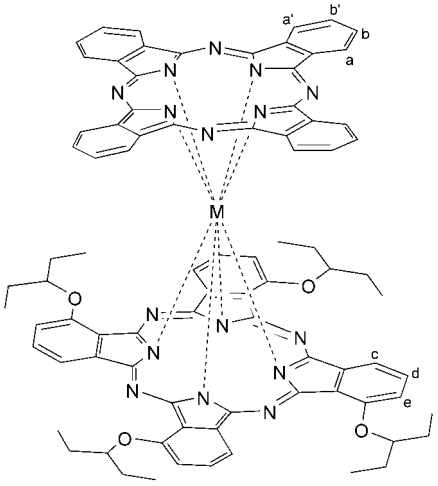

Fig. 1. *Schematic structure of the heteroleptic rare earth double-decker complexes [M^{III}(pc){pc(α-$OC_5H_{11})_4$}]* **1**–**11**. M = Y, Sm–Lu; pc = phthalocyaninato; pc(α-$OC_5H_{11})_4$ = 1,8,15,22-tetrakis(1-ethylpropoxy)phthalocyaninato.

chemistry. Due to the C_{4h} symmetry of the pc(α-$OC_5H_{11})_4$ ring and the sandwich-like structure, these molecules are intrinsically chiral possessing a C_4 symmetry[1]).

Results and Discussion. – *Synthesis of [M^{III}(pc){pc(α-$OC_5H_{11})_4$}]* 1–11. Three synthetic pathways have been reported to prepare rare earth(III) double-decker complexes with two different kinds of phthalocyaninato ligands, *i.e.*, of [M^{III}(pc′)(pc″)]. The first method involves a mixed condensation of the two corresponding phthalonitrile (= benzene-1,2-dicarbonitrile) precursors in the presence of a metal salt [9]. Obviously, this method is not practically useful because of the difficulties in separating the statistical mixtures of differently substituted bis(phthalocyaninato) complexes. The second pathway involves the treatment of [M(acac)$_3$]·*n* H_2O with two different phthalocyaninato complexes [Li_2(pc′)] and [Li_2(pc″)] [10][11]. As expected, this procedure leads to a substantial amount of homoleptic double-deckers [M^{III}(pc′)$_2$] and [M^{III}(pc″)$_2$] as by-products. The third route employs the half-sandwich complexes [M^{III}(pc′)(acac)] as the template, which induces cyclic tetramerization of the other phthalonitrile in the presence of DBU [12][13]. This pathway is also a convenient and efficient method to prepare other mixed-ring double-deckers, including [M^{III}(pc′)(por)] [14] and [M^{III}(nc′)(por)] [15] (nc′ = general naphthalocyaninato, por = general porphyrinato). In the present work, we employed the last methodology using [M^{III}(pc)(acac)] (M = Y, Sm–Lu), generated from the corresponding [M(acac)$_3$]·*n* H_2O (M = Y, Sm–Lu) and phthalonitrile, as the template. Reaction with 3-(2-ethylpropoxy)phthalonitrile in the presence of DBU in refluxing pentanol led to the heteroleptic double-deckers [M^{III}(pc){pc(α-$OC_5H_{11})_4$}] **1**–**11** in 15–31% yield. Interestingly, although cyclization of 3-substituted phthalonitriles usually gives a mixture of four constitutional isomers (with C_{4h}, D_{2h}, C_{2v}, and C_s symmetry) of tetra-α-substituted phthalocyanines [16], only the double-deckers **1**–**11** that have a C_4 symmetry could be isolated in the present case. It seems that the half-sandwich template can have some

[1]) Part of the results have been communicated [8].

control on the cyclization and complexation processes. Compounds **1**–**11** could also be prepared by treating [M^{III}(pc)(acac)] (M = Y, Sm–Lu) with the metal-free phthalocyanine H_2[pc(α-$OC_5H_{11})_4$] in refluxing octanol. The reaction yields were comparable with those obtained by using the former procedure.

The reaction yields of these compounds (15–31%) were slightly dependent on the size of the metal center. The yield was lower for a double-decker with a larger metal center (see *Table S1* in the *Appendix*). In fact, no neutral heteroleptic double-deckers could be isolated for M = La, Pr, and Nd. Attempts to prepare these compounds by using both of the above procedures led to the isolation of a trace amount of the reduced protonated double-deckers [HM^{III}(pc){pc(α-$OC_5H_{11})_4$}] (M = La, Pr, Nd) as shown by absorption spectroscopy. These results are in accord with the trend observed for [M^{III}(pc′)$_2$] (pc′ = phthalocyaninato or 2,3,9,10,16,17,23,24-octakis(octyloxy)phthalocyaninato) [17], but a reverse trend was observed for [M^{III}{nc(*t*Bu)$_4$}$_2$] (nc(*t*Bu)$_4$ = 3(4),12(13),21(22),30(31)-tetra(*tert*-butyl)-2,3-naphthalocyaninato) [18] and [M^{III}(por)$_2$] (por = *meso*-tetraphenylporphyrinato, octaethylporphyrinato) [19].

Spectroscopic Characterization. All the new heteroleptic double-deckers **1**–**11** were fully characterized by elemental analysis and various spectroscopic methods. *Table S1* (see *Appendix*) summarizes the analytical and mass-spectroscopic data. The MALDI-TOF mass spectra of these compounds clearly showed intense signals for the molecular ion M^+ or protonated molecular ion $[M+H]^+$. The isotopic pattern closely resembled the simulated one as exemplified by the spectrum of the Er analogue **8** (see *Fig. S1* in the *Appendix*).

Like the other bis(tetrapyrrolato) rare earth(III) complexes [4], double-deckers **1**–**11** can be regarded as single-hole complexes in which an unpaired electron is present in one of the macrocyclic ligands. This was demonstrated by the room-temperature EPR spectra of [M^{III}(pc){pc(α-$OC_5H_{11})_4$}] (M = Y, Lu) (*Fig. S2* in the *Appendix*), which showed a characteristic signal for organic radicals at $g = 1.997-1.998$. The signal exhibited a poorly-resolved hyperfine structure, probably due to a coupling with the N and metal nuclei, and was slightly broader for the Lu analogue **11** than for the Y counterpart **6** (peak-to-peak separation = 11.3 *vs.* 4.8 G). Lowering the temperature of **6** to 77 K led to a slight sharpening of the signal (peak-to-peak separation = 4.2 G) but the hyperfine structure remained unresolved.

Due to the presence of the unpaired electron and the paramagnetic nature of some of the rare earth ions, NMR data for such single-hole complexes are difficult to obtain. However, upon addition of hydrazine hydrate as a reducing agent, well-resolved ^{1}H-NMR spectra could be obtained for the reduced form of [M^{III}(pc){pc(α-$OC_5H_{11})_4$}] (M = Sm (**1**), Eu (**2**), Y (**6**), Lu (**11**)), in which both the macrocyclic ligands become diamagnetic dianions (*i.e.*, [M^{III}(pc^{2-}){pc(α-$OC_5H_{11})_4^{2-}$}]$^-$). *Fig. 2* shows the ^{1}H-NMR spectrum of the reduced form of **11**, which is similar to the spectra of the other three complex anions. Due to the C_4 symmetry of the molecule, the tetrasubstituted-phthalocyaninato protons (c, d, and e; see *Fig. 1*) resonate at δ 8.38 (*d*), 7.85 (*t*), and 7.44 (*d*), respectively. Interestingly, the α protons (a and a′) of the unsubstituted pc are no longer equivalent in the present environment, giving 2 *m* at δ 8.82–8.85 and 8.77–8.80, while the β protons (b and b′) give a *m* at δ 7.92–7.95. Because of the diastereotopic nature, the CH_2 protons resonate as 3 *m* at δ 2.30–2.39, 2.11–2.21, and 1.90–1.99 in a 1:1:2 ratio. Two well-resolved *t* at δ 1.39 and 1.00 are also shown for the

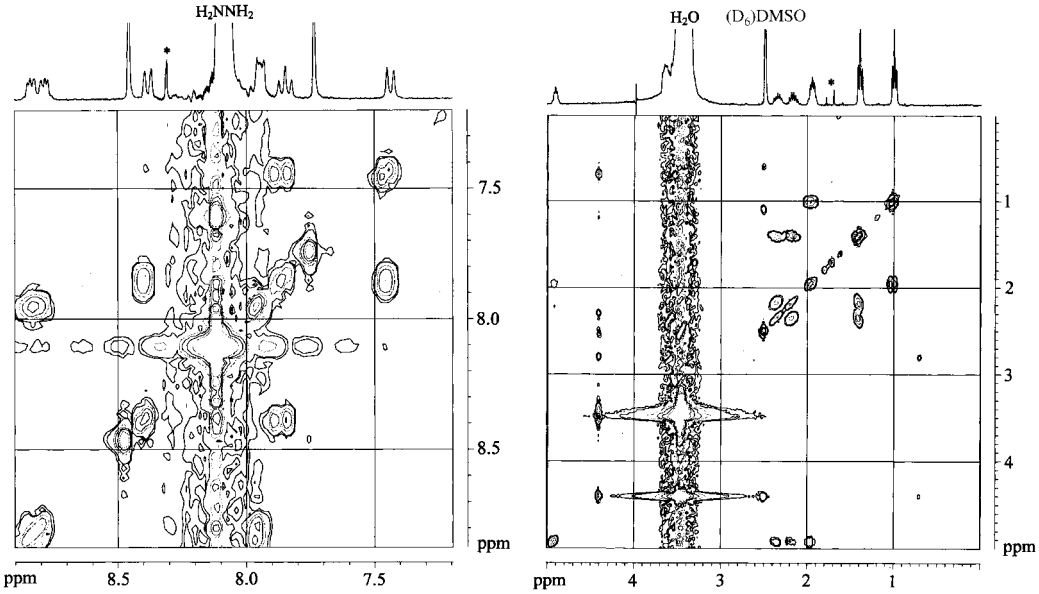

Fig. 2. *^{1}H,^{1}H-COSY Spectra of [Lu^{III}(pc){pc(α-OC$_5$H$_{11}$)$_4$}]* (**11**) *in CDCl$_3$/(D$_6$)DMSO 1:1 containing ca. 10% of hydrazine hydrate* (* indicates impurities)

Me protons. The above assignment is supported by the two-dimensional ^{1}H,^{1}H-COSY plot, from which the connectivity among the coupled protons can be unambiguously established. The remaining three double-deckers show similar spectral features (see *Table S2* in the *Appendix*).

The electronic-absorption data of this series of compounds were measured in $CHCl_3$ (see *Table 1*). The dependence of the spectral features on the metal center is illustrated with the spectra of the Sm, Tb, and Lu analogues (*Fig. 3*). All the spectra of **1** – **11** show a typical B band at *ca.* 320 nm with a shoulder at the higher-energy side. The slight splitting of this band has been observed previously for both homoleptic and heteroleptic bis(phthalocyaninato) rare earth(III) complexes [10b][12][17b]. Interestingly, the Q bands for these compounds are also split, giving three strong absorptions at 616 – 630, 645 – 662, and 685 – 702 nm, due to the lowering of molecular symmetry. In addition, two weak π-radical-anion bands at 440 – 455 and 920 – 932 nm, together with a near-IR band at 1561 – 1805 nm are also seen. The latter band is highly characteristic for rare earth(III) double-deckers which contain a hole in one of the ligands [4]. Except for the B band at *ca.* 320 nm, the absorption positions of all the remaining bands are sensitive to the metal center. Along with the lanthanide contraction, some bands shift gradually to the red, while the others are blue-shifted. *Fig. S3* (see *Appendix*) plots the wavenumber of the longest-wavelength Q band (685 – 702 nm) of **1** – **11** as a function of the ionic radius of M^{III}. A linear relationship is obtained with the wavenumber of the absorption increasing as the size of the metal center decreases. Apart from the position, the appearance of the electronic spectra is also sensitive to the metal. As shown in

Table 1. *Electronic Absorption Data for Double-Deckers* **1**–**11** *in* $CHCl_3$

	λ_{max} /nm (log ε)								
1	293 (4.66)	321 (4.88)	440 (4.19)	630 (4.77)	662 (4.71)	702 (4.74)	920 (3.26)		1805 (3.98)
2	293 (4.74)	322 (4.96)	442 (4.24)	629 (4.83)	661 (4.77)	699 (4.84)	925 (3.38)		1762 (4.03)
3	293 (4.77)	321 (4.99)	442 (4.28)	626 (4.85)	658 (4.77)	697 (4.93)	925 (3.48)		1723 (4.11)
4	293 (4.77)	320 (4.98)	443 (4.28)	624 (4.84)	654 (4.74)	695 (4.98)	928 (3.61)	1455 (3.74)	1670 (4.14)
5	293 (4.85)	320 (5.07)	445 (4.35)	622 (4.92)	653 (4.81)	693 (5.10)	928 (3.72)	1455 (3.93)	1629 (4.23)
6	293 (4.83)	320 (5.04)	446 (4.31)	621 (4.88)	652 (4.76)	691 (5.09)	930 (3.72)	1456 (3.97)	1621 (4.21)
7	293 (4.81)	321 (5.02)	448 (4.28)	621 (4.86)	651 (4.74)	691 (5.08)	931 (3.70)	1455 (3.97)	1609 (4.18)
8	293 (4.82)	321 (5.04)	449 (4.29)	620 (4.87)	649 (4.74)	689 (5.12)	930 (3.74)	1455 (4.06)	1597 (4.20)
9	293 (4.78)	320 (4.99)	450 (4.24)	618 (4.82)	647 (4.67)	688 (5.10)	930 (3.72)	1448 (4.08)	1580 (4.14)
10	293 (4.81)	320 (5.03)	454 (4.27)	617 (4.85)	646 (4.68)	687 (5.16)	932 (3.78)	1445 (4.16)	1571 (4.15)
11	293 (4.68)	320 (4.90)	455 (4.13)	616 (4.71)	645 (4.54)	685 (5.04)	932 (3.64)	1440 (4.05)	1561 (3.98)

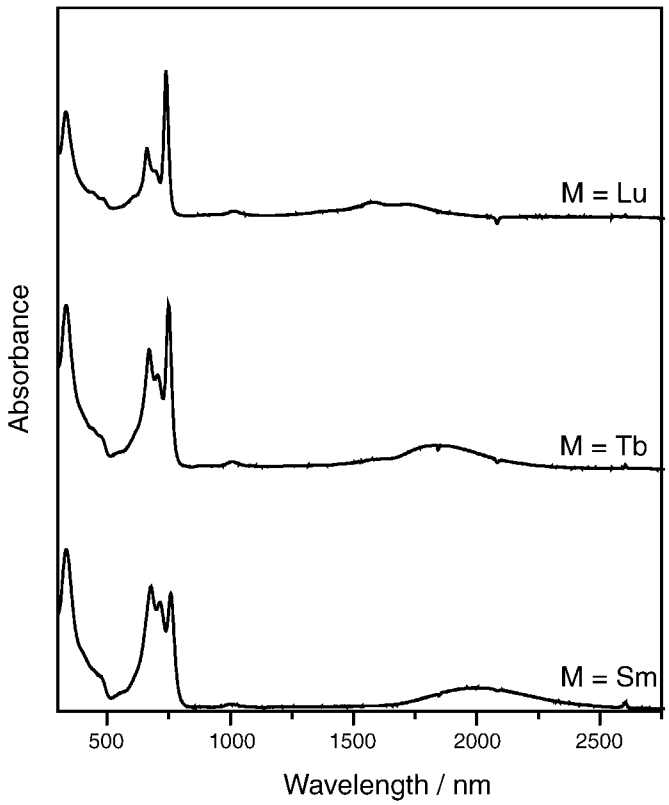

Fig. 3. *Electronic-absorption spectra of* $[M^{III}(pc)\{pc(\alpha\text{-}OC_5H_{11})_4\}]$ (M = Sm, Tb, Lu) *in* $CHCl_3$

Fig. 3, the longest-wavelength Q band becomes more intense compared with the other two Q bands as the size of the metal center decreases.

Fig. 4 shows a simplified molecular-orbital diagram of $[M^{III}(pc)\{pc(\alpha\text{-}OC_5H_{11})_4\}]$ constructed from the a_{1u} and e_g orbitals of the two ligands [20]. Due to the electron-releasing 2-ethylpropoxy groups, both the a_{1u} and e_g orbitals of $pc(\alpha\text{-}OC_5H_{11})_4$ are

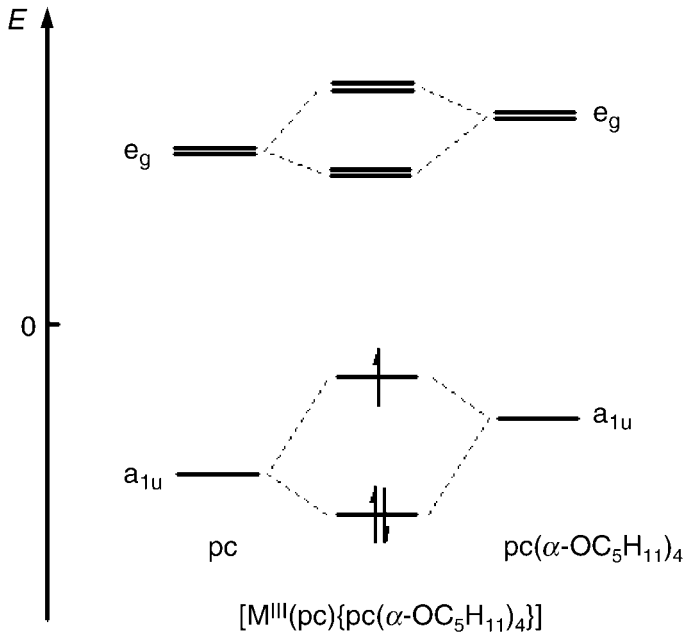

Fig. 4. *Simplified molecular-orbital diagram for [M^{III}(pc){pc(α-OC_5H_{11})$_4$}]*

higher in energy than those of pc. An unpaired electron is present in the highest semi-occupied orbital, which resembles the a_{1u} orbital of pc(α-OC_5H_{11})$_4$, leading to some unique spectral features. The weak absorption at 920–932 nm, which shifts slightly to the red with decreasing metal-ion radius, is due to the electronic transition from the semi-occupied orbital to the degenerate LUMO. The lowest-energy near-IR absorption at 1561–1805 nm is due to the transition from the second-highest occupied orbital to the semi-occupied orbital[2]). The energy involved reflects the extent of electronic coupling between the two macrocycles, which increases as the size of the metal center decreases. As mentioned above, the weak absorption at 440–455 nm is also a π-radical band, which is slightly metal-dependent (*Table 1*). This absorption can be attributed to the electronic transition from a low-lying occupied molecular orbital to the semi-occupied molecular orbital.

The presence of an unpaired electron in one of the phthalocyaninato ligands (preferentially in pc(α-OC_5H_{11})$_4$ as shown in *Fig. 4*) was supported by IR spectroscopy. An intense IR band at 1312–1318 cm^{-1} was observed for the whole series of [M^{III}(pc){pc(α-OC_5H_{11})$_4$}]. This band, which is also seen in many other single-hole phthalocyaninato-containing double-deckers, serves as a marker for the phthalocyanine radical anion [22].

---

[2]) According to the supermolecular MO model, this characteristic absorption can be attributed to the electronic transition from the second-highest-filled supermolecular bonding orbital to the half-filled supermolecular antibonding orbital (see [21]).

Structural Studies. Single crystals of $[M^{III}(pc)\{pc(\alpha\text{-}OC_5H_{11})_4\}]$ **1**, **2**, and **8** (M = Sm, Eu, and Er, resp.) suitable for X-ray diffraction analysis were obtained by slow diffusion of hexane into the corresponding $CHCl_3$ solutions. These represent the first heteroleptic bis(phthalocyaninato)metal complexes to have been structurally characterized. These compounds crystallize in the monoclinic system with two pairs of enantiomeric double-deckers per unit cell. Attempts to resolve the two enantiomers of the europium analogue **2** by HPLC (silica-gel column coated with cellulose 2,3,6-tris(3,5-dimethylphenylcarbamate) were not successful due to their limited solubility in hexane-containing solvent systems [23]. *Fig. 5* shows the molecular structure of the

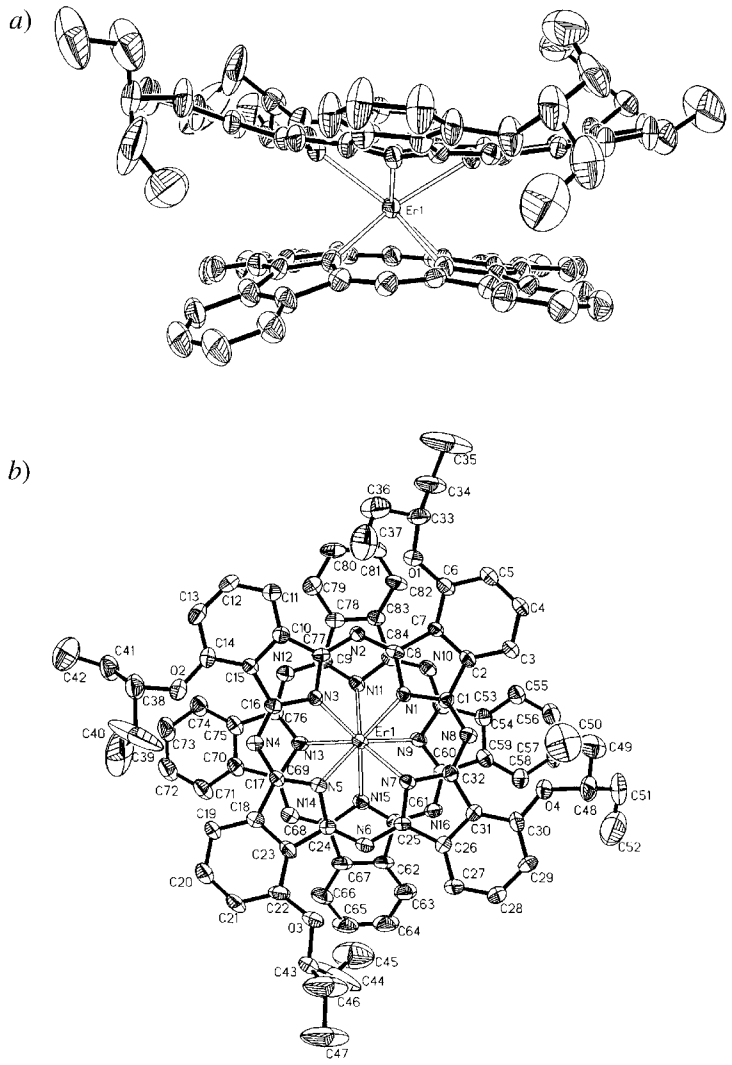

Fig. 5. *Molecular structure of* $[Er^{III}(pc)\{pc(\alpha\text{-}OC_5H_{11})_4\}]$ (**8**) *in two different perspective views showing the 30% probability thermal ellipsoids for all non-H-atoms.* Arbitrary numbering.

erbium analogue **8** in two different perspective views. The Er-center is octacoordinated by the isoindole N-atoms of the two phthalocyaninato ligands, forming a slightly distorted square antiprism. The two N_4 mean planes are virtually parallel (dihedral angle $= 0.2^\circ$) with a plane-to-plane separation of 2.708 Å. The Er-atom lies almost in the center (1.360 Å (from pc(α-OC_5H_{11})$_4$) *vs.* 1.349 Å (from pc)). Like the structures of many double-decker complexes [4], the two ligands are not planar and display a saucer shape. *Table 2* summarizes the structural parameters of the three compounds **1**, **2**, and **8**. As expected, the interplanar separation and the average M–N distances decrease with the size of the metal center. However, the extent of ligand deformation, as defined by the average dihedral angle φ of the individual isoindole rings with respect to the corresponding N_4 mean plane, remains essentially unchanged. For this series of complexes, the value of φ is slightly larger for pc(α-OC_5H_{11})$_4$ than for pc showing that the former macrocycle is slightly more deformed than the latter, probably due to the four bulky 2-ethylpropoxy substituents. The average twist angle, which is defined as the rotation angle of one macrocycle away from the eclipsed conformation of the two macrocycles, or simply the dihedral angle N(pc)-center(pc N_4 plane)-center(pc(α-OC_5H_{11})$_4$ N_4 plane)-N(pc(α-OC_5H_{11})$_4$), is close to 45° for all these complexes, showing that the two ligands are almost fully staggered. This is in line with the results obtained for [M(nc)(oep)] (nc = 2,3-naphthalocyaninato, oep = 2,3,7,8,12,13,17,18-octaethylporphyrinato) [15c][24].

Table 2. *Comparison of the Structural Data for Double-Deckers* **1**, **2**, *and* **8**

	1	**2**	**8**
Average M–N(pc) bond distance [Å]	2.4422(6)	2.4251(2)	2.3910(11)
Average M–N[pc(α-OC_5H_{11})$_4$] bond distance [Å]	2.4706(5)	2.4400(2)	2.4026(12)
M–N_4(pc) plane distance [Å]	1.411	1.403	1.349
M–N_4[pc(α-OC_5H_{11})$_4$] plane distance [Å]	1.465	1.439	1.360
Interplanar distance [Å]	2.876	2.842	2.708
Dihedral angle between the two N_4 planes [°]	1.2	1.3	0.2
Average dihedral angle φ for pc [°][a])	10.3	10.1	10.8
Average dihedral angle φ for pc(α-OC_5H_{11})$_4$ [°][a])	10.9	10.9	13.2
Average twist angle [°][b])	47.6	47.2	44.7

[a]) The average dihedral angle of the individual isoindole rings with respect to the corresponding N_4 mean plane.
[b]) Defined as the rotation angle of one macrocycle away from the eclipsed conformation of the two macrocycles.

Electrochemical Properties. The redox behavior of the heteroleptic double-deckers **1**–**11** was studied by cyclic voltammetry (CV) and differential pulse voltammetry (DPV) in CH_2Cl_2. Except for the yttrium analogue **6**, all the compounds exhibited three quasi-reversible one-electron oxidations and four quasi-reversible one-electron reductions, which can be attributed to the successive removal of electrons from and addition of electrons to the ligand-based orbitals, respectively, as the trivalent rare earth metal center cannot be oxidized or reduced under the present conditions. *Fig. 6* shows the voltammograms for [Eu^{III}(pc){pc(α-OC_5H_{11})$_4$}] (**2**), which are typical for the other rare earth counterparts. *Table 3* collects the half-wave potentials of all these processes for all the double-deckers. Like many other series of double-deckers [4][15c][17b], these potentials depend linearly on the ionic radius of the metal center

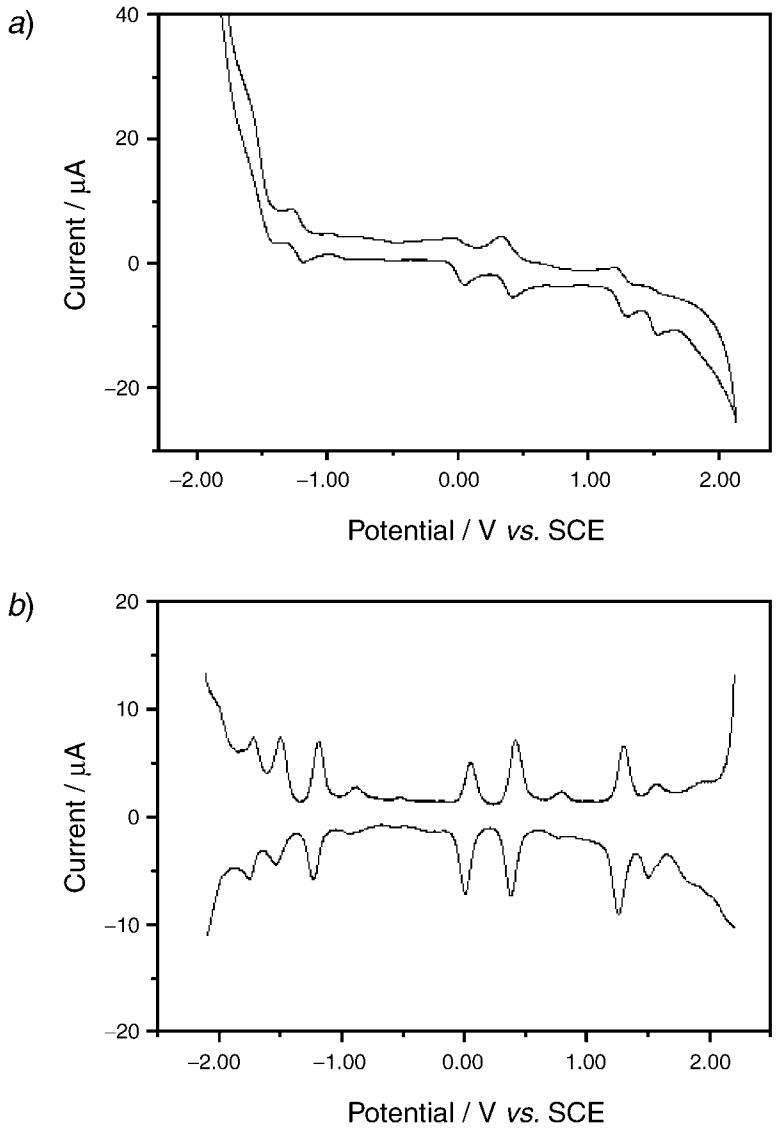

Fig. 6. a) *Cyclic voltammogram and* b) *differential pulse voltammogram of* $[Eu^{III}(pc)\{pc(\alpha\text{-}OC_5H_{11})_4\}]$ (**2**) *in* CH_2Cl_2 *containing 0.1*M $[Bu_4N][ClO_4]$ *at a scan rate of 20 and 10 mV* s^{-1}, *respectively*

(see *Fig. S4* in the *Appendix*). The first oxidation (O_1) and the first reduction (R_1) processes involve the semi-occupied orbital, while the second and the third oxidations (O_2 and O_3) involve the second-highest occupied orbital (see *Fig. 4*). As shown in *Fig. S4* (see *Appendix*), the half-wave potentials for the former two processes decrease as the size of the metal center becomes smaller, while a reverse trend is shown for the latter two processes. These results indicate that, along with the lanthanide contraction,

Table 3. *Electrochemical Data for Double-Deckers* **1**–**11**[a])

	O_3	O_2	O_1	R_1	R_2	R_3	R_4	$\Delta E_{1/2}$[b])	$\Delta E'_{1/2}$[c])	$\Delta E''_{1/2}$[d])
1	+1.46	+1.23	+0.38	0.00	−1.25	−1.52	−1.77[e])	0.38	0.85	1.25
2	+1.53	+1.28	+0.39	+0.02	−1.22	−1.52[e])	−1.74[e])	0.37	0.89	1.24
3	+1.49	+1.24	+0.35	−0.02	−1.26[e])	−1.58[e])	−1.84	0.37	0.89	1.24
4	+1.51	+1.27	+0.32	−0.03	−1.27	−1.57[e])	−1.82[e])	0.35	0.95	1.24
5	+1.56	+1.35	+0.35	−0.03	−1.24	−1.56[e])	−1.88[e])	0.38	1.00	1.21
6	–	+1.32	+0.30	−0.08	−1.27	−1.62	–	0.38	1.02	1.19
7	+1.55	+1.36	+0.32	−0.05	−1.23[e])	−1.56[e])	−1.88[e])	0.37	1.04	1.18
8	+1.61	+1.37	+0.33	−0.06	−1.23[e])	−1.60[e])	−1.88[e])	0.39	1.04	1.17
9	+1.60	+1.37	+0.32	−0.07	−1.23	−1.57[e])	−1.87[e])	0.39	1.08	1.16
10	+1.60[e])	+1.38	+0.30	−0.09	−1.23	−1.56[e])	−1.85[e])	0.39	1.08	1.14
11	+1.59	+1.38	+0.29	−0.09	−1.22[e])	−1.55[e])	−1.84[e])	0.38	1.09	1.13

[a]) Recorded with 0.1M $[Bu_4N][ClO_4]$ in CH_2Cl_2 as electrolyte at r.t. Potentials were obtained by cyclic voltammetry with a scan rate of 20 mV s^{-1} and are expressed as half-wave potentials $E_{1/2}$ in V relative to SCE unless otherwise stated. [b]) $\Delta E_{1/2} = O_1 - R_1$. [c]) $\Delta E'_{1/2} = O_2 - O_1$. [d]) $\Delta E''_{1/2} = R_1 - R_2$. [e]) By differential pulse voltammetry with a scan rate of 10 mV s^{-1}.

the semi-occupied orbital increases in energy while the energy level of the second-highest occupied orbital is lower. The increase in energy gap between these two orbitals is in accord with the blue shift of the longest-wavelength near-IR band. The potentials for the remaining three reduction processes (R_2, R_3, and R_4) are not so sensitive to the ionic radius of the metal center, suggesting that the energy level of the LUMO as well as the second-lowest unoccupied orbital remain relatively constant for the whole series. Therefore, the energy difference between the semi-occupied orbital and the second-lowest unoccupied orbital (as well as the LUMO) diminishes across the series, while that between the second-highest occupied orbital and the LUMO follows an opposite trend. These two transitions are commonly believed to be the origin of the Q bands for single-hole double-decker complexes [20]. As shown in *Table 1*, all the three Q bands are blue-shifted as the size of the metal center decreases. This suggests that these absorptions may arise mainly from the electronic transition from the second-highest occupied orbital to the LUMO for this series of complexes.

As shown in *Table 3*, the potential difference between R_1 and R_2 ($\Delta E''_{1/2}$), which represents the HOMO–LUMO gap, decreases from 1.25 V (for M = Sm) to 1.13 V (for M = Lu), whereas the gap between O_2 and O_1 ($\Delta E'_{1/2}$), which reflects the energy separation between the semi-occupied orbital and the second-highest HOMO, increases from 0.85 V (for M = Sm) to 1.09 (for M = Lu). These values should be related to the positions of the corresponding electronic transitions (*i.e.*, the absorptions at 920–932 and 1561–1805 nm, respectively). In fact, the opposite trend observed for these two cases in electrochemical studies is in good agreement with that observed in the electronic-absorption spectroscopic investigation (*Table 1*).

The potential difference between O_1 and R_1 ($\Delta E_{1/2}$) for all the heteroleptic double-deckers **1**–**11** is very similar. The values (0.35–0.39 V) are somewhat smaller than those observed for the homoleptic analogues with unsubstituted or octa(alkoxy)-phthalocyaninato ligands (0.41–0.46 V) [25]. The results suggest that these novel heteroleptic bis(phthalocyaninato) rare earth complexes should be good molecular semi-conductors and may find applications in molecular electronics [9a][26].

In summary, we prepared a novel series of heteroleptic bis(phthalocyaninato) rare earth complexes $[M^{III}(pc)\{pc(\alpha\text{-}OC_5H_{11})_4\}]$ (M = Y, Sm–Lu) as racemic mixtures. The compounds were fully characterized with various spectroscopic and electrochemical methods. The molecular structures of three of these double-deckers were also determined, confirming a C_4 symmetry. Introduction of a $pc(\alpha\text{-}OC_5H_{11})_4$ ligand to the sandwich structure induces not only chirality in the resulting double-deckers, but also significant changes in the spectroscopic and electrochemical properties.

We thank Prof. *Nagao Kobayashi* and Prof. *Hung-Kay Lee* for attempting the optical resolution of **2** and recording the EPR spectra of **6** and **11**, respectively. Financial support from the *National Science Foundation of China* (grant No. 20171028, 20325105), *National Ministry of Science and Technology of China* (grant No. 2001CB6105-04), *Ministry of Education of China*, Shandong University, and The Chinese University of Hong Kong is gratefully acknowledged.

Experimental Part

General. Pentanol and octanol were distilled from Na. Hexane used for chromatography was distilled from anh. $CaCl_2$. CH_2Cl_2 for voltammetric studies was freshly distilled from CaH_2 under N_2. All other reagents and solvents were used as received. The compounds 3-(2-ethylpropoxy)phthalonitrile [27], $H_2[pc(\alpha\text{-}OC_5H_{11})_4]$ [28], $[M(acac)_3]\cdot n\ H_2O$ [29], and $[Li_2(pc)]$ [30] were prepared according to the literature procedures. Column chromatography (CC): silica gel 60 (*Merck*; 70–230 mesh).

Electronic absorption spectra: *Hitachi U-4100* spectrophotometer. IR Spectra: KBr pellets; *Biorad-FTS-165* spectrometer with 2-cm^{-1} resolution. MALDI-TOF-MS: *Bruker BIFLEX-III* ultra-high-resolution *Fourier*-transform ion-cyclotron-resonance (FT-ICR) mass spectrometer; α-cyano-4-hydroxycinnamic acid as matrix. Elemental analyses were performed by the Institute of Chemistry, Chinese Academy of Sciences.

Voltammetry: BAS CV-50W Voltammetric analyzer, cell comprising inlets for a glassy C-disk working electrode of 2.0-mm diameter and an Ag-wire counter electrode. The Ag/Ag^+ reference electrode was connected to the soln. by a *Luggin* capillary whose tip was placed close to the working electrode. It was corrected for junction potentials by being referenced internally to the ferrocenium/ferrocene (Fe^+/Fe) couple ($E_{1/2}(Fe^+/Fe) = 501$ mV *vs.* SCE). Typically, 0.1M $[Bu_4N][ClO_4]$ in CH_2Cl_2 containing 0.5M sample was purged with N_2 for 10 min, then the voltammograms were recorded at r.t. The scan rates were 20 and 10 mV s^{-1} for CV and DPV, respectively.

Double-Decker Complexes **1**–**11**. In a typical procedure, a mixture of $[M(acac)_3]\cdot n\ H_2O$ (M = Y, Sm–Lu) (25 mg, ca. 0.05 mmol) and phthalonitrile (26 mg, 0.20 mmol) in pentanol (4 ml) was heated at 100° under N_2 for ca. 2 h. The mixture was evaporated and the residue was subjected to CC (silica gel, slowly 2 → 20% MeOH/$CHCl_3$). The obtained half-sandwich complex $[M^{III}(pc)(acac)]$ was further purified by recrystallization from CH_2Cl_2/MeOH. The half-sandwich complex $[M^{III}(pc)(acac)]$ (40 mg, ca. 0.05 mmol) was then treated with 3-(2-ethylpropoxy)phthalonitrile (50 mg, 0.23 mmol) and DBU (0.03 ml, 0.20 mmol) in refluxing pentanol (4 ml) for 12 h, or with the metal-free phthalocyanine $H_2[pc(\alpha\text{-}OC_5H_{11})_4]$ (43 mg, 0.05 mmol) in refluxing octanol (5 ml) for 8 h. After being cooled to r.t., the mixture was evaporated and the residue subjected to CC (silica gel, $CHCl_3$). Following two green fractions containing a small amount of $H_2[pc(\alpha\text{-}OC_5H_{11})_4]$ and $[M^{III}(pc)_2]$, a blue band containing the target heteroleptic double-deckers $[M^{III}(pc)\{pc(\alpha\text{-}OC_5H_{11})_4\}]$ was developed, which was collected and evaporated. The crude product was purified by repeated CC followed by recrystallization from $CHCl_3$/MeOH giving black needles.

*X-Ray Crystallography: Structure of [29*H,*31*H-*Phthalocyaninato(2- or 1-)*κN^{29},κN^{30},κN^{31},κN^{32}*][1,8,15,22-tetrakis(1-ethylpropoxy)-29*H,*31*H-*phthalocyaninato(1- or 2-)*κN^{29},κN^{30},κN^{31},κN^{32}*]samarium* (**1**), *[29*H,*31*H-*Phthalocyaninato(2- or 1-)*κN^{29},κN^{30},κN^{31},κN^{32}*][1,8,15,22-tetrakis(1-ethylpropoxy)-29*H,*31*H-*phthalocyaninato(1- or 2-)*κN^{29},κN^{30},κN^{31},κN^{32}*]europium* (**2**), and *[29*H,*31*H-*Phthalocyaninato(2- or 1-)*κN^{29},κN^{30},κN^{31},κN^{32}*][1,8,15,22-tetrakis(1-ethylpropoxy)-29*H,*31*H-*phthalocyaninato(1- or 2-)*κN^{29},κN^{30},κN^{31},κN^{32}*]erbium* (**8**). Crystal data and details of data collection and structure refinement are given in *Table 4*. Data were collected on a *Bruker SMART-CCD* diffractometer with a Mo-*K*α sealed tube (λ 0.71073 Å) at 293 K, using a ω-scan mode with an increment of 0.3°. Preliminary unit-cell parameters were obtained from 45 frames. Final unit-cell parameters were derived by global refinements of reflections obtained from integration of all the frame data. The collected frames were integrated by using the preliminary cell-orientation matrix. The SMART software

Table 4. *Crystallographic Data for Double-Deckers* **1**, **2**, *and* **8**

	1 · $CHCl_3$ · 2 H_2O	**2** · $CHCl_3$	**8**
Molecular formula	$C_{85}H_{77}Cl_3N_{16}O_6Sm$	$C_{85}H_{73}Cl_3EuN_{16}O_4$	$C_{84}H_{72}ErN_{16}O_4$
M_r	1675.33	1640.90	1536.84
Crystal system	monoclinic	monoclinic	monoclinic
Space group	$P2_1/n$	$P2_1/n$	$P2_1/n$
a [Å]	21.058(7)	21.0430(10)	15.580(8)
b [Å]	17.615(6)	17.4463(8)	34.143(18)
c [Å]	21.066(7)	21.0430(10)	15.580(8)
β [°]	90.000(5)	90.2620(10)	119.052(7)
U [Å^3]	7815(5)	7725.3(6)	7245(7)
Z	4	4	4
D_c [Mg m^{-3}]	1.424	1.411	1.409
μ [mm^{-1}]	0.920	0.979	1.223
Data collection range [°]	1.37 – 25.04	1.37 – 28.06	1.52 – 26.37
Reflections measured	40268	51900	42538
Independent reflections	13761 ($R_{int} = 0.0513$)	18666 ($R_{int} = 0.0847$)	14750 ($R_{int} = 0.1390$)
Parameters	973	982	931
R_1 ($I > 2\sigma(I)$)	0.1047	0.0643	0.0574
wR_2 ($I > 2\sigma(I)$)	0.2892	0.1591	0.1124
Goodness of fit	1.101	0.939	0.824

was used for collecting frames of data, indexing reflections, and determination of lattice constants, SAINT-PLUS for integration of intensity of reflections and scaling [31], SADABS for absorption correction [32], and SHELXL for space group and structure determination, refinements, graphics, and structure reporting [33].

CCDC-244116, -244117, and -210753 contain the supplementary crystallographic data for this paper. These data can be obtained free of charge *via* http://www.ccdc.cam.ac.uk/conts/retrieving.html (or from the *Cambridge Crystallographic Data Centre*, 12 Union Road, Cambridge CB2 1EZ, UK; fax: +44 1223 336033; e-mail: deposit@ccdc.cam.ac.uk).

Appendix

Table S1. *Analytical and Mass Spectroscopic Data for the Heteroleptic Double-Deckers* **1** – **11**

	Yield [%][a])	M^+ or $[M+H]^+$ [m/z][b])[c])	Analysis [%][c])		
			C	H	N
[Sm(pc){pc(α-$OC_5H_{11})_4$}] (**1**)	15	1523.4 (1523.5)[d])	65.82 (66.38)	4.83 (4.77)	14.86 (14.74)
[Eu(pc){pc(α-$OC_5H_{11})_4$}] (**2**)	18	1522.5 (1522.5)[d])	65.57 (66.31)	4.61 (4.77)	14.25 (14.73)
[Gd(pc){pc(α-$OC_5H_{11})_4$}] (**3**)	17	1527.4 (1527.5)[d])	65.48 (66.08)	4.80 (4.75)	14.70 (14.68)
[Tb(pc){pc(α-$OC_5H_{11})_4$}] (**4**)	19	1528.5 (1528.5)[d])	60.08 (60.14)[e])	4.63 (4.34)	12.50 (13.12)
[Dy(pc){pc(α-$OC_5H_{11})_4$}] (**5**)	23	1532.5 (1532.5)	64.55 (63.76)[f])	4.63 (4.59)	14.26 (14.08)
[Y(pc){pc(α-$OC_5H_{11})_4$}] (**6**)	17	1458.6 (1458.5)[d])	63.82 (62.71)[e])	4.75 (4.52)	13.98 (13.69)
[Ho(pc){pc(α-$OC_5H_{11})_4$}] (**7**)	25	1535.5 (1534.5)[d])	64.00 (63.66)[f])	4.69 (4.58)	14.21 (14.06)
[Er(pc){pc(α-$OC_5H_{11})_4$}] (**8**)	25	1536.5 (1536.5)	64.91 (65.65)	4.76 (4.72)	14.22 (14.58)
[Tm(pc){pc(α-$OC_5H_{11})_4$}] (**9**)	29	1537.4 (1537.5)	60.28 (59.79)[e])	4.38 (4.31)	13.10 (13.05)
[Yb(pc){pc(α-$OC_5H_{11})_4$}] (**10**)	27	1542.4 (1542.5)	64.07 (63.34)[f])	4.62 (4.56)	14.01 (13.99)
[Lu(pc){pc(α-$OC_5H_{11})_4$}] (**11**)	31	1544.0 (1544.5)	60.16 (59.58)[e])	4.36 (4.30)	12.84 (13.00)

[a]) From the cyclization of 3-(2-ethylpropoxy)phthalonitrile on the [M^{III}(pc)(acac)] template. [b]) By MALDI-TOF mass spectrometry. The value corresponds to the most abundant isotopic peak of the molecular ion M^+ unless otherwise stated. [c]) Calculated values given in parentheses. [d]) Mass corresponding to the most abundant isotopic peak of the protonated molecular ion MH^+. [e]) Contains 1.5 equiv. of solvated $CHCl_3$. [f]) Contains 0.5 equiv. of solvated $CHCl_3$.

Table S2. *^{1}H-NMR Chemical Shifts δ for the Reduced Form of Double-Deckers* **1**, **2**, **6**, *and* **11**[a]). δ in ppm, *J* in Hz.

	Signals of pc		Signals of pc(α-OC_5H_{11})$_4$					
	$H_{a/a'}$[b])	$H_{b/b'}$[b])	H_c[b])	H_d[b])	H_e[b])	CHO	CH_2	Me
1	8.23–8.28 (*m*, 4 H)	7.61–7.66	7.66	7.52	7.13	4.50–4.58	1.95–2.04	1.06
	8.12–8.17 (*m*, 4 H)	(*m*, 8 H)	(*d*, *J* = 7.5, 4 H)	(*t*, *J* = 7.5, 4 H)	(*d*, *J* = 7.5, 4 H)	(*m*, 4 H)	(*m*, 4 H)	(*t*, *J* = 7.5, 12 H)
							1.78–1.89	0.97
							(*m*, 12 H)	(*t*, *J* = 7.5, 12 H)
2	10.51–10.54 (*m*, 4 H)	8.53–8.57	10.16	8.46	8.00	6.08–6.20	2.51–2.62	1.26
	10.47–10.50 (*m*, 4 H)	(*m*, 8 H)	(*d*, *J* = 7.4, 4 H)	(*t*, *J* = 7.4, 4 H)	(*d*, *J* = 7.4, 4 H)	(*m*, 4 H)	(*m*, 4 H)	(*t*, *J* = 7.4, 12 H)
							2.28–2.33	0.67
							(*m*, 12 H)	(*t*, *J* = 7.4, 12 H)
6	8.81–8.85 (*m*, 4 H)	7.91–7.96	8.36	7.84	7.43	4.88–4.92	2.29–2.39	1.37
	8.75–8.80 (*m*, 4 H)	(*m*, 8 H)	(*d*, *J* = 7.5, 4 H)	(*t*, *J* = 7.5, 4 H)	(*d*, *J* = 7.5, 4 H)	(*m*, 4 H)	(*m*, 4 H)	(*t*, *J* = 7.5, 12 H)
							2.09–2.19	1.00
							(*m*, 4 H)	(*t*, *J* = 7.5, 12 H)
							1.89–2.00	
							(*m*, 8 H)	
11	8.82–8.85 (*m*, 4 H)	7.92–7.95	8.38	7.85	7.44	4.88–4.94	2.30–2.39	1.39
	8.77–8.80 (*m*, 4 H)	(*m*, 8 H)	(*d*, *J* = 7.5, 4 H)	(*t*, *J* = 7.5, 4 H)	(*d*, *J* = 7.5, 4 H)	(*m*, 4 H)	(*m*, 4 H)	(*t*, *J* = 7.4, 12 H)
							2.11–2.21	1.00
							(*m*, 4 H)	(*t*, *J* = 7.4, 12 H)
							1.90–1.99	
							(*m*, 8 H)	

[a]) Recorded in $CDCl_3$/(D_6)DMSO 1 : 1 containing *ca.* 10% (by volume) of hydrazine hydrate at 300 MHz. [b]) See *Fig. 1* for labels.

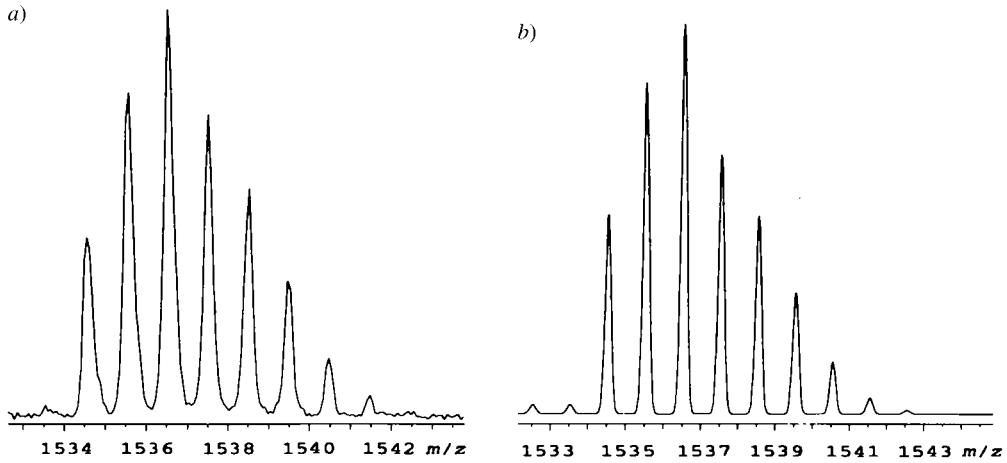

Fig. S1. a) *Experimental and* b) *simulated isotopic pattern for the molecular ion of [Er^{III}(pc){pc(α-OC_5H_{11})$_4$}]* (**8**) *in the MALDI-TOF mass spectrum*

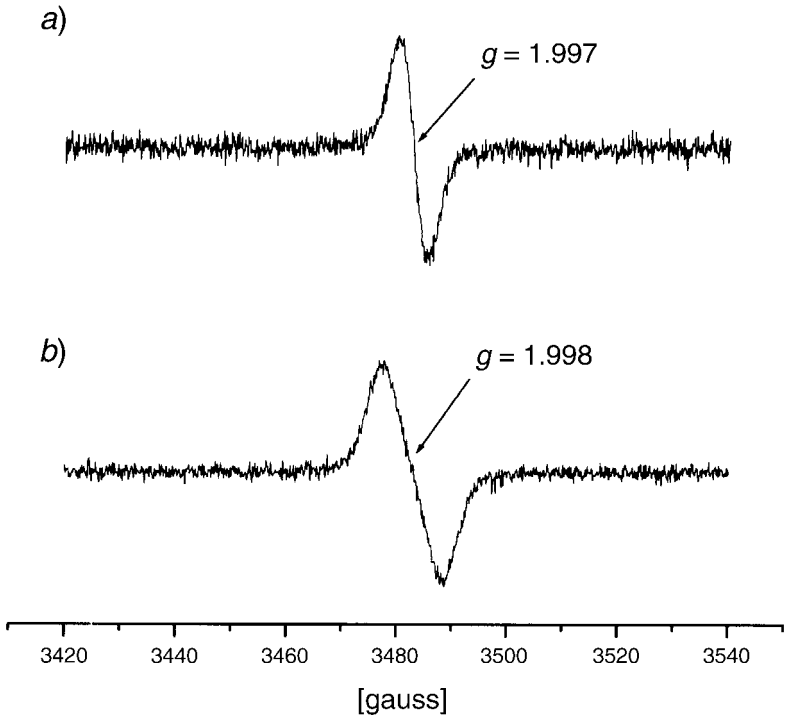

Fig. S2. *EPR Spectra* (CH_2Cl_2, r.t.) *of* a) *[Y^{III}(pc){pc(α-$OC_5H_{11})_4$}]* (**6**) *and* b) *[Lu^{III}(pc){pc-(α-$OC_5H_{11})_4$}]* (**11**)

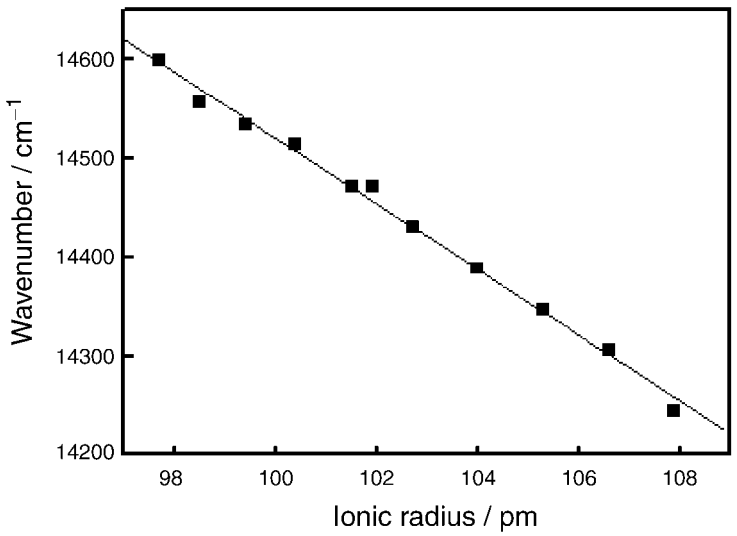

Fig. S3. *Wavenumber of the main Q band of [M^{III}(pc){pc(α-$OC_5H_{11})_4$}]* **1**–**11** *at 685–702 nm as a function of the ionic radius of M^{III}*

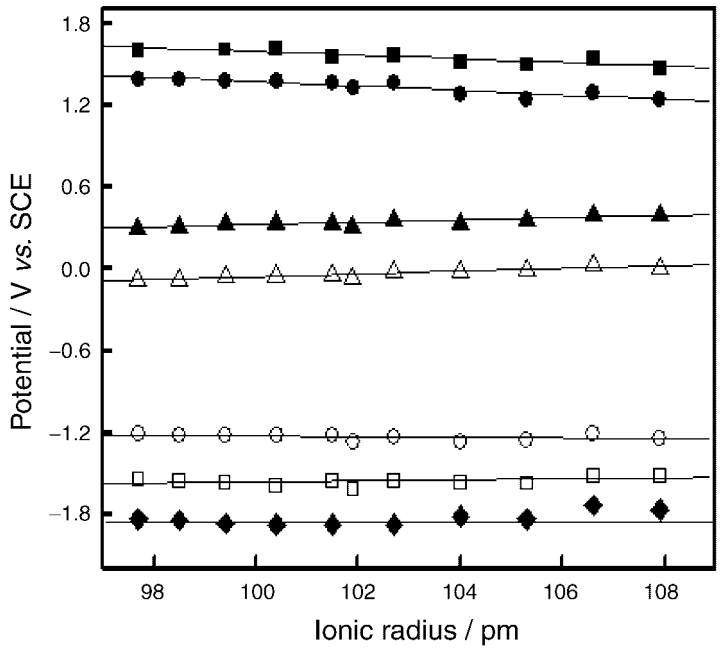

Fig. S4. *Plot of the redox potentials of [M^{III}(pc)(pc(α-$OC_5H_{11})_4$)]* **1**–**11** *as a function of the ionic radius of M^{III}.* ■ = O_3, ● = O_2, ▲ = O_1, △ = R_1, ○ = R_2, □ = R_3, ◆ = R_4.

REFERENCES

[1] T. L. Poulos, in 'The Porphyrin Handbook', Eds. K. M. Kadish, K. M. Smith, and R. Guilard, Academic Press, San Diego, 2000, Vol. 4, p. 189; H. Ogoshi, T. Mizutani, T. Hayashi, Y. Kuroda, in 'The Porphyrin Handbook', Eds. K. M. Kadish, K. M. Smith, and R. Guilard, Academic Press, San Diego, 2000, Vol. 6, p. 279; R. Paolesse, D. Monti, L. La Monica, M. Venanzi, A. Froiio, S. Nardis, C. Di Natale, E. Martinelli, A. D'Amico, *Chem.–Eur. J.* **2002**, *8*, 2476.

[2] E. Bellacchio, R. Lauceri, S. Gurrieri, L. M. Scolaro, A. Romeo, R. Purrello, *J. Am. Chem. Soc.* **1998**, *120*, 12353; E. Galardon, M. Lukas, P. Le Maux, G. Simonneaux, *Tetrahedron Lett.* **1999**, *40*, 2753; B. Boitrel, V. Baveux-Chambenoit, P. Richard, *Eur. J. Org. Chem.* **2001**, 4213; J.-L. Liang, J.-S. Huang, X.-Q. Yu, N. Zhu, C.-M. Che, *Chem.–Eur. J.* **2002**, *8*, 1563; R. Zhang, W.-Y. Yu, H.-Z. Sun, W.-S. Liu, C.-M. Che, *Chem.–Eur. J.* **2002**, *8*, 2495.

[3] H.-W. Liu, C.-F. Chen, M. Ai, A.-J. Gong, J. Jiang, F. Xi, *Tetrahedron: Asymmetry* **2000**, *11*, 4915; N. Kobayashi, *Coord. Chem. Rev.* **2001**, *219–221*, 99, and ref. cit. therein; H. Liu, Y. Liu, M. Liu, C. Chen, F. Xi, *Tetrahedron Lett.* **2001**, *42*, 7083; M. Kimura, T. Kuroda, K. Ohta, K. Hanabusa, H. Shirai, N. Kobayashi, *Langmuir* **2003**, *19*, 4825.

[4] D. K. P. Ng, J. Jiang, *Chem. Soc. Rev.* **1997**, *26*, 433; J. W. Buchler, D. K. P. Ng, in 'The Porphyrin Handbook', Eds. K. M. Kadish, K. M. Smith, R. Guilard, Academic Press, San Diego, 2000, Vol. 3, p. 245; J. Jiang, K. Kasuga, D. P. Arnold, in 'Supramolecular Photo-sensitive and Electro-active Materials', Ed. H. S. Nalwa, Academic Press, New York, 2001, p. 113; J. Jiang, W. Liu, D. P. Arnold, *J. Porphyrins Phthalocyanines* **2003**, *7*, 459.

[5] K. Tashiro, K. Konishi, T. Aida, *Angew. Chem., Int. Ed.* **1997**, *36*, 856; K. Tashiro, T. Fujiwara, K. Konishi, T. Aida, *Chem. Commun.* **1998**, 1121; K. Tashiro, K. Konishi, T. Aida, *J. Am. Chem. Soc.* **2000**, *122*, 7921.

[6] M. Takeuchi, T. Imada, S. Shinkai, *Angew. Chem., Int. Ed.* **1998**, *37*, 2096; A. Sugasaki, M. Ikeda, M. Takeuchi, A. Robertson, S. Shinkai, *J. Chem. Soc., Perkin Trans. 1* **1999**, 3259; M. Ikeda, T. Tanida, M. Takeuchi, S. Shinkai, *Org. Lett.* **2000**, *2*, 1803; A. Sugasaki, M. Ikeda, M. Takeuchi, S. Shinkai, *Angew. Chem., Int. Ed.* **2000**, *39*, 3839; A. Sugasaki, M. Ikeda, M. Takeuchi, K. Koumoto, S. Shinkai, *Tetrahedron*

2000, *56*, 4717; A. Robertson, M. Ikeda, M. Takeuchi, S. Shinkai, *Bull. Chem. Soc. Jpn.* **2001**, *74*, 883; M. Takeuchi, M. Ikeda, A. Sugasaki, S. Shinkai, *Acc. Chem. Res.* **2001**, *34*, 865; M. Ikeda, M. Takeuchi, S. Shinkai, F. Tani, Y. Naruta, S. Sakamoto, K. Yamaguchi, *Chem.–Eur. J.* **2002**, *8*, 5542.

[7] V. M. Negrimovskii, M. Bouvet, E. A. Luk'yanets, J. Simon, *J. Porphyrins Phthalocyanines* **2001**, *5*, 423.

[8] Y. Bian, R. Wang, J. Jiang, C.-H. Lee, J. Wang, D. K. P. Ng, *Chem. Commun.* **2003**, 1194.

[9] a) M. Bouvet, J. Simon, *Chem. Phys. Lett.* **1990**, *172*, 299; b) Y. Liu, K. Shigehara, M. Hara, A. Yamada, *J. Am. Chem. Soc.* **1991**, *113*, 440; c) L. G. Tomilova, Y. G. Gorbunova, M. L. Rodriguez-Mendez, J. A. De Saja, *Mendeleev Commun.* **1994**, 127; d) N. Ishikawa, Y. Kaizu, *Chem. Lett.* **1998**, 183.

[10] a) A. Pondaven, Y. Cozien, M. L' Her, *New J. Chem.* **1991**, *15*, 515; b) A. Pondaven, Y. Cozien, M. L' Her, *New J. Chem.* **1992**, *16*, 711; c) F. Guyon, A. Pondaven, P. Guenot, M. L' Her, *Inorg. Chem.* **1994**, *33*, 4787.

[11] N. Ishikawa, O. Ohno, K. Kaizu, *Chem. Phys. Lett.* **1991**, *180*, 51; Y. Liu, K. Shigehara, A. Yamada, *Bull. Chem. Soc. Jpn.* **1992**, *65*, 250; N. Ishikawa, K. Kaizu, *Chem. Phys. Lett.* **1993**, *203*, 472.

[12] J. Jiang, W. Liu, W.-F. Law, J. Lin, D. K. P. Ng, *Inorg. Chim. Acta* **1998**, *268*, 141; J. Jiang, J. Xie, M. T. M. Choi, Y. Yan, S. Sun, D. K. P. Ng, *J. Prophyrins Phthalocyanines* **1999**, *3*, 322.

[13] M. Bouvet, P. Bassoul, J. Simon, *Mol. Cryst. Liq. Cryst.* **1994**, *252*, 31; D. Pernin, K. Haberroth, J. Simon, *J. Chem. Soc., Perkin Trans. 1* **1997**, 1265; F. Steybe, J. Simon, *New J. Chem.* **1998**, *22*, 1305.

[14] J. Jiang, M. T. M. Choi, W.-F. Law, J. Chen, D. K. P. Ng, *Polyhedron* **1998**, *17*, 3903.

[15] a) J. Jiang, D. Du, M. T. M. Choi, J. Xie, D. K. P. Ng, *Chem. Lett.* **1999**, 261; b) J. Jiang, W. Liu, K.-L. Cheng, K.-W. Poon, D. K. P. Ng, *Eur. J. Inorg. Chem.* **2001**, 413; c) J. Jiang, Y. Bian, F. Furuya, W. Liu, M. T. M. Choi, N. Kobayashi, H.-W. Li, Q. Yang, T. C. W. Mak, D. K. P. Ng, *Chem.–Eur. J.* **2001**, *7*, 5059; d) F. Furuya, N. Kobayashi, Y. Bian, J. Jiang, *Chem. Lett.* **2001**, 944.

[16] C. Rager, G. Schmid, M. Hanack, *Chem.–Eur. J.* **1999**, *5*, 280.

[17] a) C. Clarisse, M. T. Riou, *Inorg. Chim. Acta* **1987**, *130*, 139; b) W. Liu, J. Jiang, D. Du, D. P. Arnold, *Aust. J. Chem*. **2000**, *53*, 131.

[18] J. Jiang, W. Liu, K.-W. Poon, D. Du, D. P. Arnold, D. K. P. Ng, *Eur. J. Inorg. Chem*. **2000**, 205; T. Nyokong, F. Furuya, N. Kobayashi, D. Du, W. Liu, J. Jiang, *Inorg. Chem*. **2000**, *39*, 128.

[19] J. W. Buchler, J. Hüttermann, J. Löffler, *Bull. Chem. Soc. Jpn.* **1988**, *61*, 71; J. W. Buchler, P. Hammerschmitt, I. Kaufeld, J. Löffler, *Chem. Ber.* **1991**, *124*, 2151.

[20] E. Orti, J. L. Bredas, C. Clarisse, *J. Chem. Phys.* **1990**, *92*, 1228; R. Rousseau, R. Aroca, M. L. Rodriguez-Mendez, *J. Mol. Struct.* **1995**, *356*, 49; N. Ishikawa, *J. Porphyrins Phthalocyanines* **2001**, *5*, 87.

[21] J. K. Duchowski, D. F. Bocian, *J. Am. Chem. Soc.* **1990**, *112*, 3312; O. Bilsel, J. Rodriguez, S. N. Milam, P. A. Gorlin, G. S. Girolami, K. S. Suslick, D. Holten, *J. Am. Chem. Soc.* **1992**, *114*, 6528.

[22] J. Jiang, D. P. Arnold, H. Yu, *Polyhedron* **1999**, *18*, 2129; F. Lu, M. Bao, C. Ma, X. Zhang, D. P. Arnold, J. Jiang, *Spectrochim Acta*, *Part A* **2003**, *59*, 3273.

[23] N. Kobayashi, T. Nonomura, *Tetrahedron Lett.* **2002**, *43*, 4253.

[24] Y. Bian, D. Wang, R. Wang, L. Weng, J. Dou, D. Zhao, D. K. P. Ng, J. Jiang, *New J. Chem.* **2003**, *27*, 844; Y. Bian, J. Jiang, Y. Tao, M. T. M. Choi, R. Li, A. C. H. Ng, P. Zhu, N. Pan, X. Sun, D. P. Arnold, Z. Zhou, H.-W. Li, D. K. P. Ng, *J. Am. Chem. Soc.* **2003**, *125*, 12257.

[25] P. Zhu, F. Lu, N. Pan, D. P. Arnold, S. Zhang, J. Jiang, *Eur. J. Inorg. Chem*. **2004**, 510.

[26] J. Simon, J. J. Andre, 'Molecular Semi-conductors', Springer Verlag, Berlin, 1985.

[27] W. O. Siegl, *J. Heterocycl. Chem.* **1981**, *18*, 1613.

[28] K. Kasuga, M. Kawashima, K. Asano, T. Sugimori, K. Abe, T. Kikkawa, T. Fujiwara, *Chem. Lett.* **1996**, 867.

[29] J. G. Stites, C. N. McCarty, L. L. Quill, *J. Am. Chem. Soc.* **1948**, *70*, 3142.

[30] P. A. Barrett, D. A. Frye, R. P. Linstead, *J. Chem. Soc.* **1938**, 1157.

[31] 'SMART and SAINT for Windows NT Software Reference Manuals', Version 5.0, Bruker Analytical X-Ray Systems, Madison, WI, 1997.

[32] G. M. Sheldrick, 'SADABS – A Software for Empirical Absorption Correction', University of Göttingen, Germany, 1997.

[33] 'SHELXL Reference Manual', Version 5.1, Bruker Analytical X-Ray Systems, Madison, WI, 1997.

Received April 20, 2004